Journal of Nuclear Materials 493 (2017) 303–309

Contents lists available at ScienceDirect

Journal of Nuclear Materials

journal homepage: www.elsevier.com/locate/jnucmat

Finite element analysis of ion transport in solid state nuclear waste form materials

F. Rabbi [a, *], K. Brinkman [b], J. Amoroso [c], K. Reifsnider [d]

[a] University of South Carolina, United States
[b] Clemson University, United States
[c] Savannah River National Laboratory, United States
[d] University of Texas Arlington, United States

ARTICLE INFO

Article history:
Received 13 September 2016
Received in revised form
25 May 2017
Accepted 26 May 2017
Available online 27 May 2017

Keywords:
Diffusion
COMSOL
Nernst-Planck
Waste form

ABSTRACT

Release of nuclear species from spent fuel ceramic waste form storage depends on the individual constituent properties as well as their internal morphology, heterogeneity and boundary conditions. Predicting the release rate is essential for designing a ceramic waste form, which is capable of effectively storing the spent fuel without contaminating the surrounding environment for a longer period of time. To predict the release rate, in the present work a conformal finite element model is developed based on the Nernst Planck Equation. The equation describes charged species transport through different media by convection, diffusion, or migration. And the transport can be driven by chemical/electrical potentials or velocity fields. The model calculates species flux in the waste form with different diffusion coefficient for each species in each constituent phase. In the work reported, a 2D approach is taken to investigate the contributions of different basic parameters in a waste form design, i.e., volume fraction, phase dispersion, phase surface area variation, phase diffusion co-efficient, boundary concentration etc. The analytical approach with preliminary results is discussed. The method is postulated to be a foundation for conformal analysis based design of heterogeneous waste form materials.

1. Introduction

Radioactive waste streams resulting from legacy weapons production as well as advanced commercial fuel cycles [1], present researchers with the challenge to manage the waste in an efficient and safe manner. An efficient system must have the capability to contain a radioactive material within itself and limit the release of the waste material in the surrounding environment to an allowable release rate. Among different waste form materials, SYNROC-C is a titanate based ceramic composed of four different targeted phases – zirconolite, hollandite, perovskite, and pyrochlore [2]. Different Separation processes isolate several important radionuclides that need to be sequestered including $Cs^{135/137}$, Tc^{99}, lanthanide fission products and residual actinide elements U, Pu, Am, Np^{237} [3]. To store these nuclear waste materials, different storage systems have been developed. Ceramic waste form incorporating a wider range of radionuclides has the potential to be a viable option to be used as a durable and effective medium, lowering the storage and disposal costs associated with advanced fuel cycles [4]. Flexibility of synthesis processes of ceramic waste form with varying microstructure and material phases gives the ability to design efficient storage solutions. Recent research on melt processing of waste forms has many advantages over the conventional solid-state synthesis methods and can reduce potential contamination associated with extensive powder handling operations [5]. But the influence of these microstructural variations on charge transport behavior need to be investigated to understand the contribution of these variations on overall flux of nuclides out of the system. Study by Brinkman et al. shows contribution of microstructure in overall charge transport in crystalline waste form systems [6].

To study these characteristics to design an efficient waste form, experimental methods with numerous iterations have proved to be time consuming and costly. Performance test of these systems experimentally by different leaching experiment such as Single Pass Flow Through (SPFT) Test – ASTM C1662, MCC-1, Static Leach Test – ASTM C1220, Solution Replacement Test, Product Consistency Test (PCT) – ASTM C1285 and Vapor Hydration Test (VHT) –

* Corresponding author.
E-mail address: rabbi@email.sc.edu (F. Rabbi).

http://dx.doi.org/10.1016/j.jnucmat.2017.05.039
0022-3115/

ASTM C1663 only provides information about the performance of the waste form for a short period of time in comparison to reference materials, typically standard borosilicate glass. The current suite of testing and analysis does not provide information about the mechanism of corrosion, the performance of the waste form as a function of microstructure and morphology and ultimately the performance over geological timescales.

Finite element analysis of these systems to determine optimum microstructure, phase combinations and mixture ratio can facilitate the design process by reducing time and cost. Finite element analysis is now widely used to investigate electrochemical systems [7,8]. In this work, a finite element model of waste form system is used to simulate radionuclides ion transport in the system. This model can be used to resolve both 2D and 3D domains representing ideal or real microstructures of a waste form system. Here we introduce a 2D ideal domain representing a 2-phase waste form system to investigate the contributions of different system parameters, i.e., Diffusion co-efficient ratio between phases, initial radionuclides concentration ratio between phases, volume fraction of the phases and dispersion of the secondary phases.

For this work, our choice of radionuclides is Cesium (Cs) and the Ceramic waste form structure containing Cs is Hollandite. The ideal 2D microstructure representation is motivated by the actual microstructure of a Fe-Hollandite structure fabricated by melting and crystallizing process reported by Brinkman et al. [9]. In Fig. 1, a Backscattered Electron Micrograph is showing several well-defined phases of the material with different Cs concentration. Crystalline phases determined from X-ray Diffraction XRD measurements and Energy Dispersive X-ray Spectroscopy EDAX elemental analysis. The ideal 2D microstructure used in the finite element analysis represents similar properties variations between phases, initial Cs concentration difference and geometrical structural variation seen in the real microstructure.

Cs ion flow is driven by concentration gradient between the interior and outside environment. In a ceramic composite material, charge transport can be influenced by the bulk transport behavior as well surface exchange phenomena. However, in this work we focused on the bulk transport mechanism controlled by diffusion, as suggested by Shaw et al. [10]. This mechanism is represented by the Nernst-Planck equation [11]. Here we are not considering grain boundary corrosion that will likely occur in the matrix phase and accelerate the degradation process. But this is an important parameter in the overall waste form performance. In our future investigations of both 2D and 3D conformal analysis, we will introduce contribution from grain boundary.

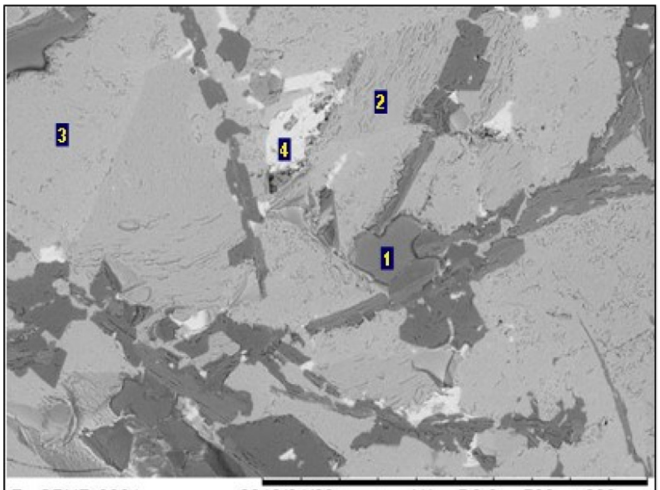

Spot	Elements (Major, Minor)	Crystalline Phases*
1	O,Al,Fe,Ti	$FeAl_2O_4$, $(A^{+3})_2TiO_5$
2,3	O,Ti,Al,Fe,Ba, (Cs)	Hollandite
4	O, Ti, Cs, Al	$Cs_2Ti_2O_5$, $CsAlTiO_4$

Fig. 1. Fe-Hollandite $Ba_{1.0}Cs_{0.3}Fe_{2.3}Ti_{5.7}O_{16}$ fabricated by melting and crystallizing backscattered electron micrograph.

2. Governing equations

To calculate the flux of stored nuclear ion through the waste form structure, we used Nernst-Planck flux equation. This equation describes transport of chemical species by convection, migration and diffusion through electrolyte membrane. Nernst-Planck equation has been used to model different charge transport phenomenon [12,13,14]. This equation has been utilized to represent charge transport in various electrochemical systems i.e. Battery [15], Fuel Cells [16] etc. The Nernst-Planck equation based model can be used to calculate concentration gradient, species flux, potential gradient of the system. Equation (1) shows Nernst-Planck equation

$$N_i = -D_i \nabla c_i - z_i u_{m,i} F c_i \nabla \phi + c_i u \tag{1}$$

N_i = Flux of species, i (mol/m^{2}s)
D_i = Diffusion co-efficient (m^2/s)
c_i = Concentration of ion, i (mol/m^3)
z_i = Valance of species
$u_{m,i}$ = mobility (s/mol/kg)
F = Faraday constant
ϕ_i = Electrolyte Potential
u = velocity vector (m/s)

In the case of a solid structure, velocity term u_i is ignored due to the absence of continuous flow through void. Migration term is ignored as no potential is applied across any of the boundaries. In this study, we also did not consider the potential difference created by the space charge due to the defects accumulated at the grain boundaries [17]. However, if required, this potential can be applied to the model using internal boundary condition. For this case of solid waste form, Cs release will be controlled by the diffusion co-efficient of the species through the waste form medium and driven by the concentration gradient of the species. The amount of Cs released can be obtained by calculating the total flux using equation (1). Transient solution of the equation calculates flux over time that can be used to obtain the leaching rate of Cs. Domain diffusion coefficient was obtained from reported ionic conductivity of Cs in hollandite structure [18]. Nernst-Einstein relation is used to calculate the diffusion co-efficient described by Equation (2) [19].

$$\sigma = \frac{z_i^2 e^2 c_i}{k_B T} D_i \tag{2}$$

Where, D_i = Diffusion co-efficient (m^2/s)
σ = Ionic Conductivity
z_i = Valance of species
c_i = Concentration of ion, i (mol/m^3)
k_B = Boltzmann's constant

3. Model description

The Nernst-Planck equation is solved using Nernst-Planck

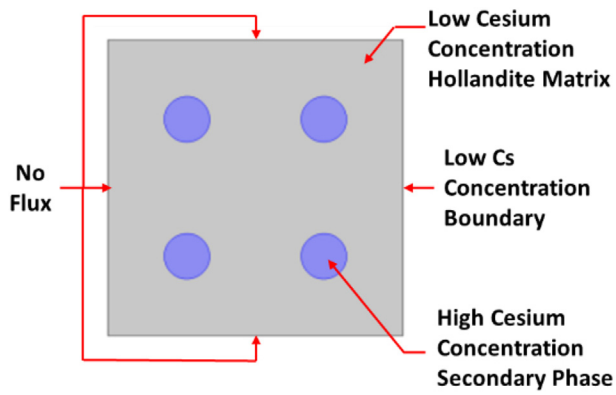

Fig. 2. 2D 2 phase waste form model structure representation with boundary condition.

Equation Module of COMSOL Multi-Physics. Both 2D and 3D structure can be used as the material domain in this model. For conformal analysis with real microstructure, computational domain can be generated form 3D scans of the material using Transmission X-ray Microscopy (TXM). Chiu et al. utilized this method to obtain 3D structural scan to investigate ceramic composite oxygen separation membrane [20]. In this Study we investigate a 2D two phase ideal waste form structure with regular geometric shapes. Fig. 2 shows 2-phases of the Cs Waste from having different Cs diffusion co-efficient and initial Cs concentration.

Top, bottom and left boundary of the system is set as blocked to prevent flow of Cs through. The right boundary of the system has a very low concentration of Cs representing open boundary condition to the environment. The Cs concentration gradient between initial internal and external surface initiates the outward diffusion of Cs. Transient solution of the model is obtained to calculate flux of Cs over time. In this study, we wanted to identify dependence of flux on relative diffusion co-efficient variations between phases as well as initial Cs concentration in each phase. We also investigated the contribution of varying volume fraction as well as dispersion of the secondary inclusion phase inside of the structure to the overall Cs leaching behavior. In this work, each waste form combination was operated over a 10-day cycle and flux data calculated at the beginning, in the middle and at the end of the cycles were presented. The 10-day time frame was selected to identify and study the influence of the above mentioned parameters in a finite time frame so that these transport behaviors can be compared to behavior obtained from leeching experiments performed in waste forms designed to degrade at a faster rate. For this study, we did not include grain boundary effect in the matrix phases. But in our future study, grain boundary contribution will be added to this model. In this model, options to apply diffusion properties can to the grain boundaries are available. It is also possible to calculate diffusion behavior of species along the grain boundaries.

To study the relative diffusion co-efficient contribution, the ratio

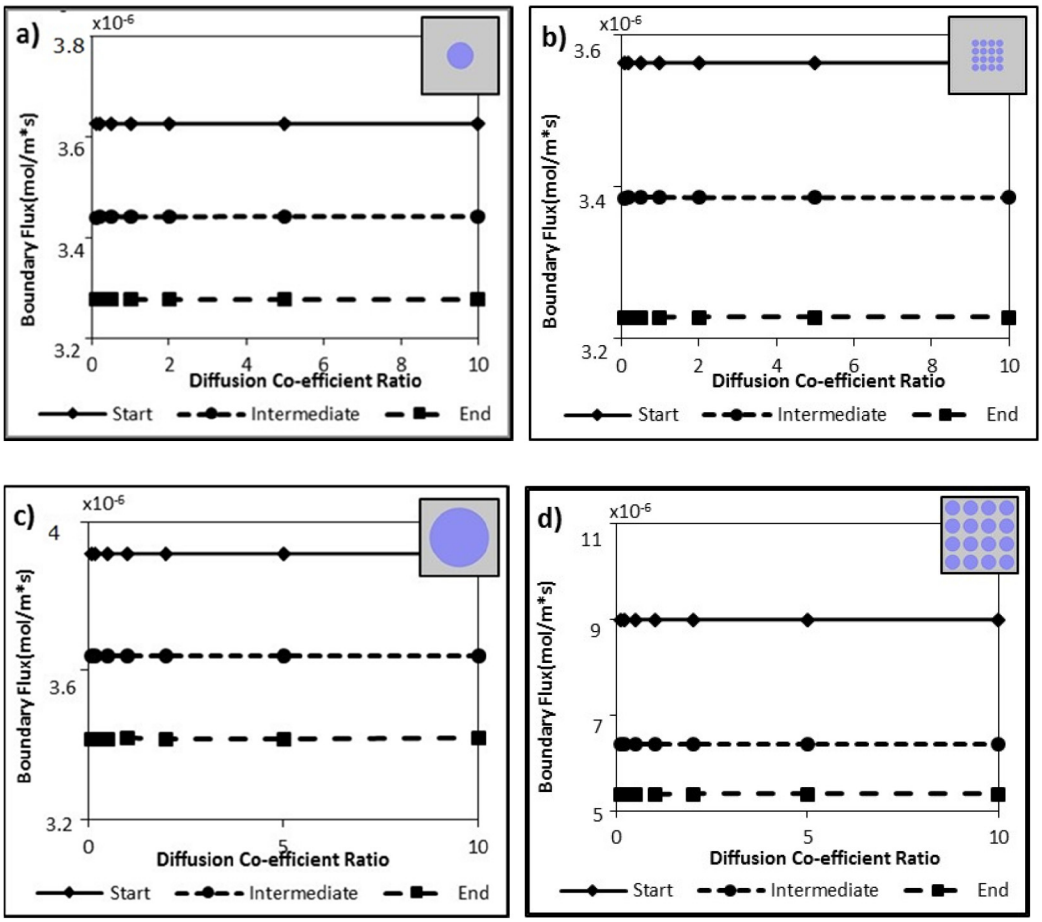

Fig. 3. Diffusion flux of Cs in open boundary vs Diffusion Co-efficient ratio between two phases for 3 stages of 10-day cycle at a) volume fraction (vf): 0.1 and No. of secondary phase inclusion: 1, b) vf: 0.1 and No. of inclusion: 16, c) vf: 0.5 and No. of inclusion: 1 and d) vf: 0.5 and No. of inclusion: 16. Inset figures show volume fraction and inclusion configuration.

between diffusion co-efficient of Cs in two phases was varied from 0.1 to 10. Similarly, to study initial Cs concentration, the ratio of the two initial conditions were varied from 0.1 to 10. Flux dependence of volume fraction was studied by varying the secondary inclusion phases from 0.1 to 0.5. To study secondary phase dispersion; for each volume fraction we had a combination of 1, 4, 9 and 16 number of elements arranged in a square distributed array. This dispersion study will demonstrate influence of varying internal surface area of the phases for same volume fraction on the overall boundary flux.

4. Result & discussion

4.1. Phase diffusion co-efficient

To study the contribution of the relative diffusion co-efficient of Cs in the two phases, we varied the diffusion co-efficient of the secondary inclusion phase relative to the external matrix phase. The ratio between the diffusion co-efficient varied from 0.1 to 10. Total boundary flux was calculated for a 10-day period. The time stages, i.e. start, intermediate and end are presented in the following figures from the calculated data.

Here Fig. 3a and b shows dependence of flux variation on Diffusion co-efficient ratio for volume fraction of 0.1 with 1 and 16 elements. In addition, Fig. 3c and d shows dependence of flux variation on Diffusion co-efficient ratio for volume fraction of 0.5 with 1 and 16 elements. For each cases with minimum and maximum volume fraction and secondary inclusion elements, we see that boundary flux does not vary at any stage of the 10-day run. This indicates that diffusion co-efficient of the secondary inclusion phase does not have a significant effect on the overall flux behavior with time.

4.2. Initial concentration variation

To study the contribution of relative initial concentration of Cs in the two phases, we varied the Cs concentration in the secondary inclusion phase relative to the external matrix phase. The ratio between the initial concentrations was varied from 0.1 to 10.

Here Fig. 4a and b shows dependence of flux variation on initial Cs concentration ratio for volume fraction of 0.1 with 1 and 16 elements. Moreover, Fig. 4c and d shows dependence of flux variation on initial Cs concentration ratio for volume fraction of 0.5 with 1 and 16 elements. For lower volume fraction, we see very small boundary flux variation in the three stages any of the 10 day run. However, for higher volume fraction observe large variation of boundary flux with increasing initial Cs concentration ratio. This indicates that initial Cs concentration of the secondary inclusion phase influences the boundary flux with increasing volume fraction.

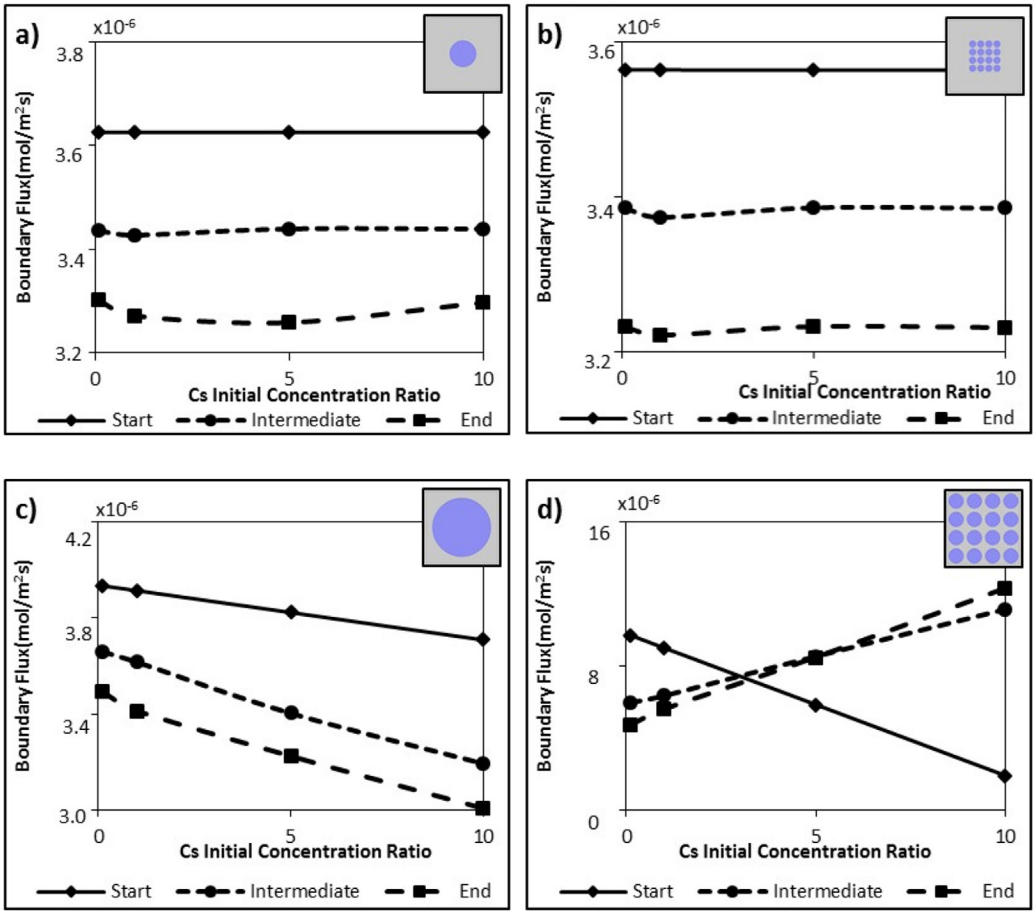

Fig. 4. Diffusion flux of Cs in open boundary vs Initial Cs concentration ratio between two phases for 3 stages of 10-day cycle at a) vf: 0.1 and No. of secondary phase inclusion: 1, b) vf: 0.1 and No. of inclusion: 16, c) vf: 0.5 and No. of inclusion: 1 and d) vf: 0.5 and No. of inclusion: 16. Inset figures show volume fraction and inclusion configuration.

4.3. Volume fraction

As we have seen that ratio of diffusion co-efficient and initial Cs concentration between phases do not contribute significantly to the overall flux, we will set the two ratios at 0.1 for our volume fraction and dispersion study.

To study the contribution of volume fraction, we varied the volume fraction of the secondary inclusion phase from 0.1 to 0.5. Fig. 5a, b, c and d shows boundary flux variation with varying volume fraction for 4 dispersion cases with 1, 4, 9 and 16 number of secondary inclusions. Here in all cases we can see that, with increasing volume fraction, the boundary flux first decreases to an intermediate lower value and then starts to increase with increasing values. This behavior is consistent throughout each case, and discussed earlier. The increasing flux with increasing volume fraction is facilitated by the lower concentration secondary region, which acts as an accelerated flow path for the Cs ion because of the concentration gradient present between the phases.

4.4. Dispersion

To study the contribution of dispersion of the inclusion phase, we varied the number of the secondary inclusion phase by 1, 4, 9 and 16. Fig. 6a, b, c and d shows boundary flux variation with varying numbers of inclusion for five volume fraction variations form 0.1–0.5. of secondary inclusions. Fig. 6a and b shows, for a lower volume fraction (0.1–0.2), the flux increases to a maximum and then decreases gradually with increasing secondary phase element numbers. But in Fig. 6c, d and e we can see that for higher value volume fraction (0.3–0.5) the flux is behaving oppositely, first decreasing and then gradually increasing with increasing element numbers. It is clear that the dispersion of the secondary (distributed) phase has a major and significant effect on the global flux out of the waste form material. It is shown that for small volume fractions of second phase, the flux drops off when the second phase is divided into more particles, whereas with higher volume fraction of second phase it increases as the (larger) second phase region is divided into smaller parts, suggesting that there are volume fraction thresholds for the influence of dispersion, and that the surface to volume ratio of the dispersed particles is very influential. In fact, there are two distinct regions of influence, the first dominated by situations where the total particle surface to control element volume ratio is small (e.g., all of the low volume fraction cases, Fig. 6a and b and the low particle number cases for high volume fraction cases, the first parts of Fig. 6c and d) and the second dominated by situations where the total particle surface to control element volume is large, as in Fig. 6e, and the later parts of Fig. 6c and d. This suggests a new design parameter, the total inclusion surface area to control volume. It is also useful to note that the extreme surface to volume ratios associated with very small particles and the particle shapes drive the Inclusion Surface to Control Volume (IS/CV) ratio. Nearly spherical particles have less influence than irregularly shaped inclusion morphologies.

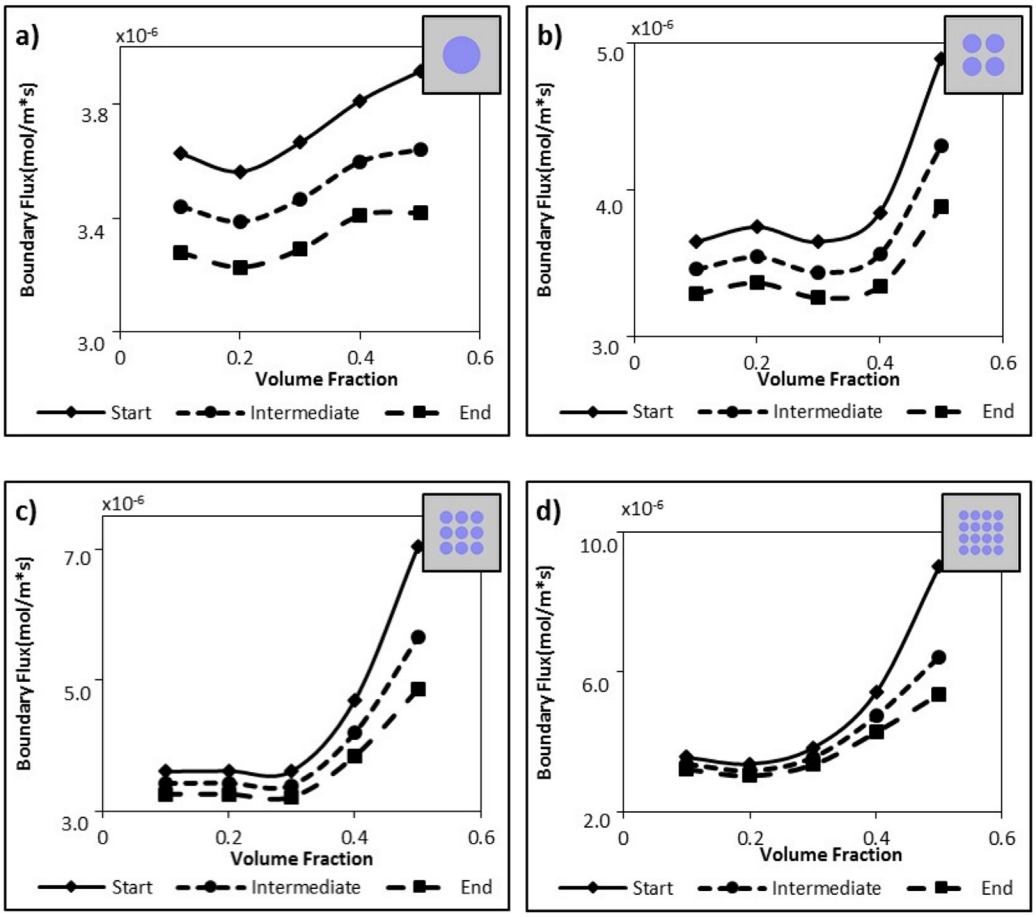

Fig. 5. Diffusion flux of Cs in the open boundary vs secondary inclusion phase volume fraction for 3 stages of 10-day cycle at a) No. of secondary phase inclusion: 1, b) No. of inclusion: 4, c) No. of inclusion: 9 and d) No. of inclusion: 16. Inset figures show inclusion configuration.

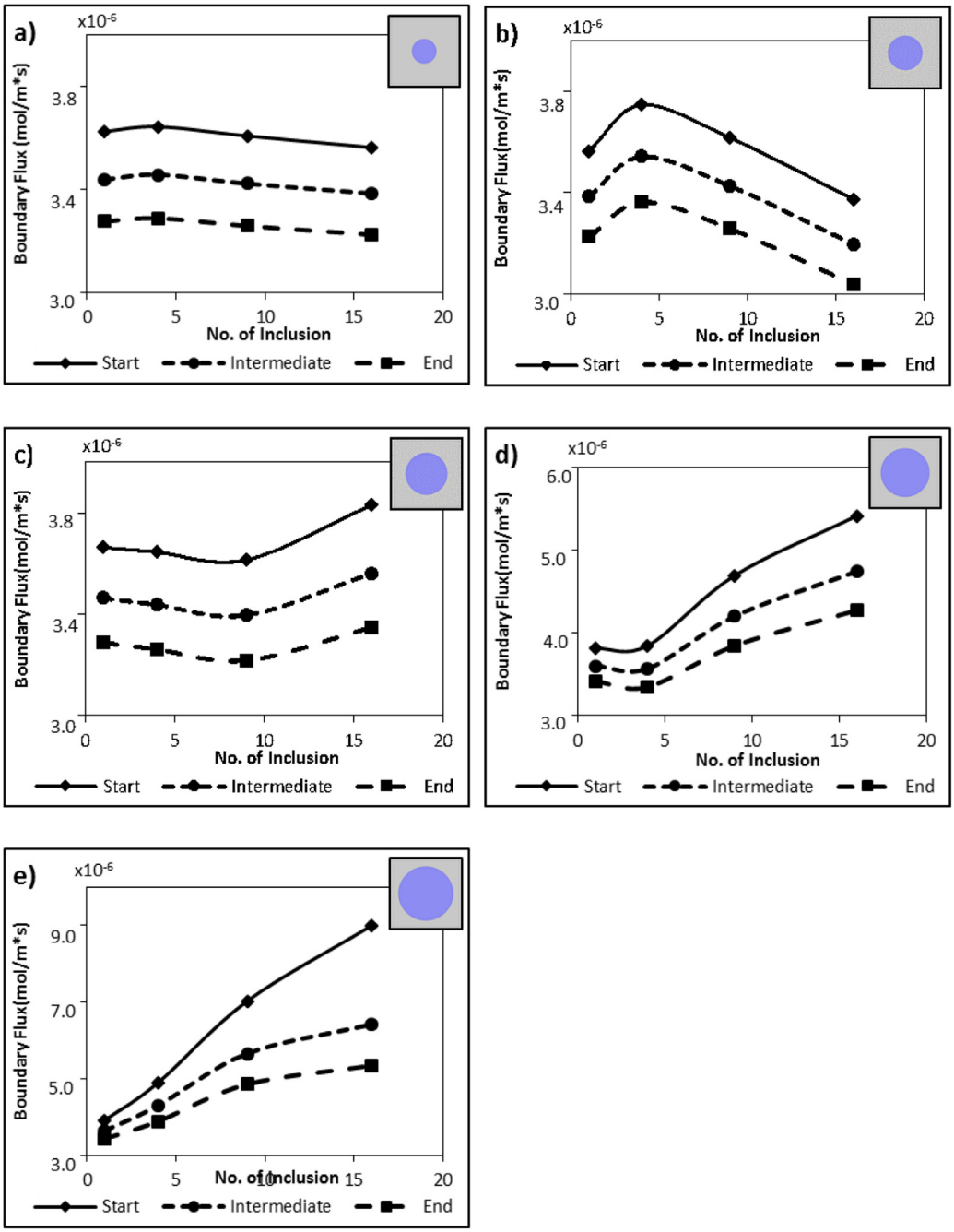

Fig. 6. Diffusion flux of Cs in open boundary vs No. of inclusion of secondary phase for 3 stages of 10-day cycle for secondary inclusion phase a) vf: 0.1, b) vf: 0.2, c) vf: 0.3, d) vf: 0.4 and e) vf: 0. Inset figures show volume fraction configuration.

5. Conclusion

We have developed a conformal multifunctional analysis method based on the Nernst Plank equation and postulated the method as a foundation for analysis - based design of heterogeneous waste form materials. The model describes charged species transport through different media by convection, diffusion, or migration, and the transport can be driven by chemical/electrical potentials or velocity fields. The model calculates species flux in the waste form with different diffusion co-efficient for each species in each constituent phase. In the work reported, a 2D approach is taken to investigate the contributions of different basic parameters in a waste form design. The influence of diffusion ratios, volume fraction of second phase, initial concentration ratios of the phases, and relative dispersion of the included phase were investigated. It was found that the dispersion of the included phase has a large and complex influence on the global flux of the material species that is to be contained. Moreover, a new design variable based on the ratio of the total surface of the included phase to the volume of the control volume is highly effective in characterizing the influence of distributed phase morphology and microstructure. Continuing work will focus on developing further understanding of this new methodology, investigating grain boundary contribution to the matrix degradation process and on extending it to 3D

representations with similar study of defects in the form of voids in the microstructure. We can predict some of the behavior we might expect to see due to the presence of void in the structure. These voids will have the lowest initial concentration of Cs and initial flow of Cs will be towards these voids beside towards the open boundary on the right hand side until an equilibrium is reached.

Acknowledgement

The authors are grateful for the support of Nuclear Energy University Program of the US Department of Energy (Award ID: DE-NE0008260).

References

[1] R.C. Ewing, W.J. Weber, F.W. Clinard, Radiation effects in nuclear waste forms for high-level radioactive waste, Prog. Nucl. Energy 29 (2) (1995) 63–127.
[2] AE Ringwood, et al., "Immobilisation of High Level Nuclear Reactor Wastes in SYNROC", 1979.
[3] Kyle S. Brinkman, et al., Crystalline Ceramic Waste Forms, Reference Formulation Report, 2012.
[4] National Research Council, Waste Forms Technology and Performance, Final Report, The National Academies Press, Washington, DC, 2011, http://www.nap.edu/catalog/13100/waste-forms-technology-and-performance-final-report.
[5] Jake Amoroso, et al., Melt processed multiphase ceramic waste forms for nuclear waste immobilization, J. Nucl. Mater. 454 (1) (2014) 12–21.
[6] Yun Xu, et al., A-Site compositional effects in Ga-Doped hollandite materials of the form BaxCsyGa2x+ yTi8-2x- yO16: implications for Cs immobilization in crystalline ceramic waste forms, Sci. Rep. 6 (2016) 27412.
[7] Sadik Kakac, Anchasa Pramuanjaroenkij, Xiang Yang Zhou, A review of numerical modeling of solid oxide fuel cells, Int. J. Hydrogen Energy 32 (7) (2007) 761–786.
[8] Atilla Bıyıkoğlu, Review of proton exchange membrane fuel cell models, Int. J. Hydrogen Energy 30 (11) (2005) 1181–1212.
[9] K. Brinkman, et al., Crystalline Ceramic Waste Forms: Comparison of Reference Process for Ceramic Waste Form Fabrication, US Department of Energy Report SRNL-STI-2013-00442 (FCRD-SWF-2013-000229), 2013.
[10] Henry F. Shaw, Determination of the Open and Closed Porosity in an Immobilized Pu Ceramic Waste Form, UCRL-ID-132605, Lawrence Livermore National Laboratory, Livermore, CA, 1998.
[11] Ramon Codina, A discontinuity-capturing crosswind-dissipation for the finite element solution of the Convection-Diffusion equation, Comput. Methods Appl. Mech. Eng. 110 (3) (1993) 325–342.
[12] Astrid Gjelstad, Knut Einar Rasmussen, Stig Pedersen-Bjergaard, Simulation of flux during electro-membrane extraction based on the Nernst–Planck equation, J. Chromatogr. A 1174 (1) (2007) 104–111.
[13] Fazle Rabbi, Kenneth L. Reifsnider, and Kyle S. Brinkman, "Multiphysics charge transport behavior study of heterogeneous functional material systems using finite element analysis of real microstructural domain", Presented at International Conference on Computational and Experimental Engineering and Sciences, Reno, NV, no. July, 2015 (n.d.).
[14] Fazle Rabbi, Kenneth L. Reifsnider, and Kyle S. Brinkman, "Heterogeneous materials design for sustainable nuclear waste storage using life prediction by conformal finite element analysis", Presented at REWAS 2016: Towards Materials Resource Sustainability, 2016, 203.
[15] Adam Z. Weber, et al., Redox flow batteries: a review, J. Appl. Electrochem. 41 (10) (2011) 1137–1164.
[16] Denver Cheddie, Norman Munroe, Review and comparison of approaches to proton exchange membrane fuel cell modeling, J. Power Sources 147 (1) (2005) 72–84.
[17] David R. Diercks, et al., Three-dimensional quantification of composition and electrostatic potential at individual grain boundaries in doped ceria, J. Mater. Chem. A 4 (14) (2016) 5167–5175.
[18] A.Y. Leinekugel-le-Cocq, et al., Synthesis and characterization of hollandite-type material intended for the specific containment of radioactive Cesium, J. Solid State Chem. 179 (10) (2006) 3196–3208.
[19] Paul J. Gellings, H.J. Bouwmeester, Handbook of Solid State Electrochemistry, CRC press, 1997.
[20] William M. Harris, et al., Characterization of 3D interconnected microstructural network in mixed ionic and electronic conducting ceramic composites, Nanoscale 6 (9) (2014) 4480–4485.